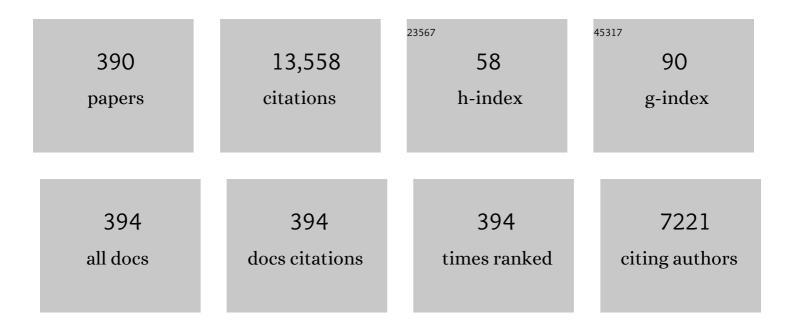
List of Publications by Year in descending order

Source: https://exaly.com/author-pdf/4852669/publications.pdf Version: 2024-02-01



#	Article	IF	CITATIONS
1	Two-dimensional molybdenum carbide (MXene) as an efficient nanoadditive for achieving superlubricity under ultrahigh pressure. Friction, 2023, 11, 369-382.	6.4	18
2	Extremely low friction on gold surface with surfactant molecules induced by surface potential. Friction, 2023, 11, 513-523.	6.4	3
3	Dynamic friction energy dissipation and enhanced contrast in high frequency bimodal atomic force microscopy. Friction, 2022, 10, 748-761.	6.4	8
4	Temperature-controlled Friction Coefficient Lubricated by Liquid Crystal. Liquid Crystals, 2022, 49, 66-71.	2.2	0
5	A smart healable anticorrosion coating with enhanced loading of benzotriazole enabled by ultra-highly exfoliated graphene and mussel-inspired chemistry. Carbon, 2022, 187, 439-450.	10.3	13
6	Wear in-situ self-healing polymer composites incorporated with bifunctional microcapsules. Composites Part B: Engineering, 2022, 232, 109566.	12.0	25
7	The relationship between surface structure and super-lubrication performance based on 2D MOFs. Applied Materials Today, 2022, 26, 101382.	4.3	7
8	Macroscale superlubricity under ultrahigh contact pressure in the presence of layered double hydroxide nanosheets. Nano Research, 2022, 15, 4700-4709.	10.4	9
9	Fluctuation of Interfacial Electronic Properties Induces Friction Tuning under an Electric Field. Nano Letters, 2022, 22, 1889-1896.	9.1	23
10	Coupling effect of boundary tribofilm and hydrodynamic film. Cell Reports Physical Science, 2022, 3, 100778.	5.6	6
11	High-quality ultra-flat reduced graphene oxide nanosheets with super-robust lubrication performances. Chemical Engineering Journal, 2022, 438, 135620.	12.7	19
12	Preparation and Tribological Properties of Self-Lubricating Epoxy Resins with Oil-Containing Nanocapsules. ACS Applied Materials & amp; Interfaces, 2022, 14, 18954-18964.	8.0	16
13	Coupled Optimization of Groove Texture for Parallel Ring–Ring Friction Pairs: Theory and Experiments. Tribology Letters, 2022, 70, 1.	2.6	8
14	Visualizing ultrafast defectâ€controlled interlayer electronâ€phonon coupling in van der Waals heterostructures. Advanced Materials, 2022, , 2106955.	21.0	1
15	Controllable group tailoring enables enhanced pH-responsive behaviors of polydopamine delivery system in smart self-healing anticorrosion coatings. Progress in Organic Coatings, 2022, 170, 106989.	3.9	3
16	Modified graphene as novel lubricating additive with high dispersion stability in oil. Friction, 2021, 9, 143-154.	6.4	45
17	Tribological behavior of layered double hydroxides with various chemical compositions and morphologies as grease additives. Friction, 2021, 9, 952-962.	6.4	35
18	An investigation on the tribological behaviors of steel/copper and steel/steel friction pairs via lubrication with a graphene additive. Friction, 2021, 9, 228-238.	6.4	33

#	Article	IF	CITATIONS
19	Micro/atomic-scale vibration induced superlubricity. Friction, 2021, 9, 1163-1174.	6.4	16
20	Vibration-induced superlubricity. , 2021, , 53-70.		0
21	Toward micro- and nanoscale robust superlubricity by 2D materials. , 2021, , 131-144.		1
22	Energy dissipation through phonon and electron behaviors of superlubricity in 2D materials. , 2021, , 145-166.		0
23	Liquid superlubricity with 2D material additives. , 2021, , 167-187.		1
24	Tribo-induced interfacial nanostructures stimulating superlubricity in amorphous carbon films. , 2021, , 289-307.		0
25	Superlubricity of water-based lubricants. , 2021, , 333-357.		1
26	Superlubricity with nonaqueous liquid. , 2021, , 379-403.		3
27	Exploration of molecular behaviors in liquid superlubricity. , 2021, , 475-498.		Ο
28	Influence of a carbon-based tribofilm induced by the friction temperature on the tribological properties of impregnated graphite sliding against a cemented carbide. Friction, 2021, 9, 686-696.	6.4	26
29	A simple method to understand molecular conformation on surface-enhanced Raman scattering substrate. Journal of Molecular Structure, 2021, 1223, 128908.	3.6	2
30	In-situ formation of tribofilm with Ti3C2Tx MXene nanoflakes triggers macroscale superlubricity. Tribology International, 2021, 154, 106695.	5.9	64
31	Superlubricity of black phosphorus as lubricant additive. , 2021, , 439-460.		Ο
32	Unraveling the Friction Evolution Mechanism of Diamondâ€Like Carbon Film during Nanoscale Runningâ€In Process toward Superlubricity. Small, 2021, 17, e2005607.	10.0	21
33	Tribochemical mechanism of superlubricity in graphene quantum dots modified DLC films under high contact pressure. Carbon, 2021, 173, 329-338.	10.3	38
34	Influence of structural evolution on sliding interface for enhancing tribological performance of onion-like carbon films via thermal annealing. Applied Surface Science, 2021, 541, 148441.	6.1	14
35	Improvement of the lubrication properties of grease with Mn3O4/graphene (Mn3O4#G) nanocomposite additive. Friction, 2021, 9, 1361-1377.	6.4	23
36	A review on tribology of polymer composite coatings. Friction, 2021, 9, 429-470.	6.4	95

#	Article	IF	CITATIONS
37	Ultralow friction polymer composites incorporated with monodispersed oil microcapsules. Friction, 2021, 9, 29-40.	6.4	45
38	Superlubricity under ultrahigh contact pressure enabled by partially oxidized black phosphorus nanosheets. Npj 2D Materials and Applications, 2021, 5, .	7.9	40
39	The transients in the evaporation of sessile liquid droplets and the applicability of the steady-state approximation. International Journal of Heat and Mass Transfer, 2021, 169, 120946.	4.8	2
40	In situ synthesis of Mn3O4/graphene nanocomposite and its application as a lubrication additive at high temperatures. Applied Surface Science, 2021, 546, 149019.	6.1	27
41	Macroscale superlubricity of Si-doped diamond-like carbon film enabled by graphene oxide as additives. Carbon, 2021, 176, 358-366.	10.3	48
42	Shear-Induced Interfacial Structural Conversion Triggers Macroscale Superlubricity: From Black Phosphorus Nanoflakes to Phosphorus Oxide. ACS Applied Materials & Interfaces, 2021, 13, 31947-31956.	8.0	33
43	Fast Opticalâ€Thermal Responsive Intelligent Glass Realized by Hydrated Poly(N â€Isopropylacrylamide) Film. Macromolecular Materials and Engineering, 2021, 306, 2100272.	3.6	0
44	Light-Controlled Friction by Carboxylic Azobenzene Molecular Self-Assembly Layers. Frontiers in Chemistry, 2021, 9, 707232.	3.6	4
45	Origin of friction and the new frictionless technology—Superlubricity: Advancements and future outlook. Nano Energy, 2021, 86, 106092.	16.0	93
46	Preparation of Triple-Functionalized Montmorillonite Layers Promoting Thermal Stability of Polystyrene. Nanomaterials, 2021, 11, 2170.	4.1	4
47	Hexadecane-containing sandwich structure based triboelectric nanogenerator with remarkable performance enhancement. Nano Energy, 2021, 87, 106198.	16.0	40
48	Influence of "Seebeck effect" on charge transfer between two friction surfaces. Tribology International, 2021, 161, 107060.	5.9	2
49	Temporary or permanent liquid superlubricity failure depending on shear-induced evolution of surface topography. Tribology International, 2021, 161, 107076.	5.9	17
50	2D metal-organic frameworks with square grid structure: A promising new-generation superlubricating material. Nano Today, 2021, 40, 101262.	11.9	42
51	Magnetic field effect on apparent viscosity reducing of different crude oils at low temperature. Colloids and Surfaces A: Physicochemical and Engineering Aspects, 2021, 629, 127372.	4.7	12
52	Efficient one-pot synthesis of mussel-inspired Cu-doped polydopamine nanoparticles with enhanced lubrication under heavy loads. Chemical Engineering Journal, 2021, 426, 131287.	12.7	23
53	Thermal-mechanical fully coupled analysis of high-speed angular contact ball bearings. Journal of Mechanical Science and Technology, 2021, 35, 669-678.	1.5	7
54	Optimization of groove texture profile to improve hydrodynamic lubrication performance: Theory and experiments. Friction, 2020, 8, 83-94.	6.4	65

#	Article	IF	CITATIONS
55	Synthesis and characterizations of zwitterionic copolymer hydrogels with excellent lubrication behavior. Tribology International, 2020, 143, 106026.	5.9	33
56	Modelling for water-based liquid lubrication with ultra-low friction coefficient in rough surface point contact. Tribology International, 2020, 141, 105901.	5.9	18
57	Understanding Interlayer Contact Conductance in Twisted Bilayer Graphene. Small, 2020, 16, e1902844.	10.0	27
58	Tribo-Induced Interfacial Material Transfer of an Atomic Force Microscopy Probe Assisting Superlubricity in a WS ₂ /Graphene Heterojunction. ACS Applied Materials & Interfaces, 2020, 12, 4031-4040.	8.0	35
59	Macroscale superlubricity achieved between zwitterionic copolymer hydrogel and sapphire in water. Materials and Design, 2020, 188, 108441.	7.0	30
60	Ultrastable Lubricating Properties of Robust Self-Repairing Tribofilms Enabled by in Situ-Assembled Polydopamine Nanoparticles. Langmuir, 2020, 36, 852-861.	3.5	31
61	Origins of Superlubricity Promoted by Hydrated Multivalent Ions. Journal of Physical Chemistry Letters, 2020, 11, 184-190.	4.6	47
62	Catalytically Active Oil-Based Lubricant Additives Enabled by Calcining Ni–Al Layered Double Hydroxides. Journal of Physical Chemistry Letters, 2020, 11, 113-120.	4.6	31
63	Dynamic wear sensor array based on single-electrode triboelectric nanogenerators. Nano Energy, 2020, 68, 104303.	16.0	18
64	Direct Visualization of Exciton Transport in Defective Few‣ayer WS ₂ by Ultrafast Microscopy. Advanced Materials, 2020, 32, e1906540.	21.0	50
65	Potential-Dependent Friction on a Graphitic Surface in Ionic Solution. Journal of Physical Chemistry C, 2020, 124, 23745-23751.	3.1	11
66	Intelligent lubricating materials: A review. Composites Part B: Engineering, 2020, 202, 108450.	12.0	89
67	Influence Factors on Mechanisms of Superlubricity in DLC Films: A Review. Frontiers in Mechanical Engineering, 2020, 6, .	1.8	33
68	Superlubricity between Graphite Layers in Ultrahigh Vacuum. ACS Applied Materials & Interfaces, 2020, 12, 43167-43172.	8.0	43
69	Preparation and tribological properties of PTFE/DE/ATF6 composites with self-contained solid-liquid synergetic lubricating performance. Composites Communications, 2020, 22, 100513.	6.3	14
70	Black Phosphorus Quantum Dots in Aqueous Ethylene Glycol for Macroscale Superlubricity. ACS Applied Nano Materials, 2020, 3, 4799-4809.	5.0	50
71	Macroscale Light-Controlled Lubrication Enabled by Introducing Diarylethene Molecules in a Nanoconfinement. Langmuir, 2020, 36, 5820-5828.	3.5	10
72	Preparation and tribological properties of solid-liquid synergetic self-lubricating PTFE/SiO2/PAO6 composites. Composites Part B: Engineering, 2020, 196, 108133.	12.0	39

#	Article	IF	CITATIONS
73	Enhancement of friction performance of fluorinated graphene and molybdenum disulfide coating by microdimple arrays. Carbon, 2020, 167, 122-131.	10.3	32
74	A highly tough and ultralow friction resin nanocomposite with crosslinkable polymer-encapsulated nanoparticles. Composites Part B: Engineering, 2020, 197, 108157.	12.0	25
75	Superlubricitive engineering—Future industry nearly getting rid of wear and frictional energy consumption. Friction, 2020, 8, 643-665.	6.4	142
76	Mechanical and tribological properties of nanocomposites incorporated with two-dimensional materials. Friction, 2020, 8, 813-846.	6.4	79
77	Band Structure, Band Offsets, and Intrinsic Defect Properties of Few-Layer Arsenic and Antimony. Journal of Physical Chemistry C, 2020, 124, 7441-7448.	3.1	9
78	Graphene-induced reconstruction of the sliding interface assisting the improved lubricity of various tribo-couples. Materials and Design, 2020, 191, 108661.	7.0	23
79	Achieving a superlubricating ohmic sliding electrical contact <i>via</i> a 2D heterointerface: a computational investigation. Nanoscale, 2020, 12, 7857-7863.	5.6	11
80	Influence of elastic property on the friction between atomic force microscope tips and 2D materials. Nanotechnology, 2020, 31, 285710.	2.6	14
81	Controllable Superlubricity System of Polyalkylene Glycol Aqueous Solutions under Various Applied Conditions. Macromolecular Materials and Engineering, 2020, 305, 2000141.	3.6	13
82	Superlubrication obtained with mixtures of hydrated ions and polyethylene glycol solutions in the mixed and hydrodynamic lubrication regimes. Journal of Colloid and Interface Science, 2020, 579, 479-488.	9.4	39
83	Effect of deformation modes and heat treatment on microstructure and impact property restoration of internal crack healing in SA 508 steel. Materials Science & Engineering A: Structural Materials: Properties, Microstructure and Processing, 2020, 778, 139073.	5.6	11
84	Achieving controllable friction of ultrafine-grained graphite HPG510 by tailoring the interfacial nanostructures. Applied Surface Science, 2020, 512, 145731.	6.1	8
85	Super-Slippery Degraded Black Phosphorus/Silicon Dioxide Interface. ACS Applied Materials & Interfaces, 2020, 12, 7717-7726.	8.0	46
86	Microscale superlubricity at multiple gold–graphite heterointerfaces under ambient conditions. Carbon, 2020, 161, 827-833.	10.3	18
87	Nanostructured tribolayer-dependent lubricity of graphene and modified graphene nanoflakes on sliding steel surfaces in humid air. Tribology International, 2020, 145, 106203.	5.9	20
88	Study on microstructural and tribological properties of sulphonitrocarburized layers diffused by hollow cathode discharging. Vacuum, 2020, 174, 109188.	3.5	7
89	Electrical bearing failures in electric vehicles. Friction, 2020, 8, 4-28.	6.4	97
90	Tribo-Induced Near-Infrared Light Emission between Metal and Quartz. Langmuir, 2020, 36, 1165-1173.	3.5	1

#	Article	IF	CITATIONS
91	Fabrication of a graphene layer probe to measure force interactions in layered heterojunctions. Nanoscale, 2020, 12, 5435-5443.	5.6	17
92	Superhigh-exfoliation graphene with a unique two-dimensional (2D) microstructure for lubrication application. Applied Surface Science, 2020, 513, 145608.	6.1	30
93	A molecular dynamics study of lubricating mechanism of graphene nanoflakes embedded in Cu-based nanocomposite. Applied Surface Science, 2020, 511, 145620.	6.1	29
94	Interfacial Nanostructure of 2D Ti ₃ C ₂ /Graphene Quantum Dots Hybrid Multicoating for Ultralow Wear. Advanced Engineering Materials, 2020, 22, 1901369.	3.5	34
95	The Effects of Homogenizing and Quenching and Tempering Treatments on Crack Healing. Metals, 2020, 10, 427.	2.3	4
96	Macroscale Superlubricity Achieved on the Hydrophobic Graphene Coating with Glycerol. ACS Applied Materials & Interfaces, 2020, 12, 18859-18869.	8.0	51
97	Atomic-scale insights into the interfacial instability of superlubricity in hydrogenated amorphous carbon films. Science Advances, 2020, 6, eaay1272.	10.3	61
98	Exploring interlayer interaction of SnSe2 by low-frequency Raman spectroscopy. Physica E: Low-Dimensional Systems and Nanostructures, 2019, 105, 7-12.	2.7	8
99	Tangential motion mechanism and reverse hydrodynamic effects of acoustic platform with nonparallel squeeze film. Proceedings of the Institution of Mechanical Engineers, Part J: Journal of Engineering Tribology, 2019, 233, 194-204.	1.8	1
100	Thinning of glycerol in the presence of multi-walled carbon nanotubes. Journal of Chemical Physics, 2019, 151, 054302.	3.0	2
101	Enhancement of friction performance enabled by a synergetic effect between graphene oxide and molybdenum disulfide. Carbon, 2019, 154, 266-276.	10.3	64
102	Cationic Surfactant Micelles Lubricate Graphitic Surface in Water. Langmuir, 2019, 35, 11108-11113.	3.5	10
103	Zwitterionic Hydrogel Incorporated Graphene Oxide Nanosheets with Improved Strength and Lubricity. Langmuir, 2019, 35, 11452-11462.	3.5	40
104	Ultra-Wear-Resistant MXene-Based Composite Coating via in Situ Formed Nanostructured Tribofilm. ACS Applied Materials & Interfaces, 2019, 11, 32569-32576.	8.0	82
105	Temperature measurement during the sliding between Al2O3 and SiO2 crystals by double line of Atomic Emission Spectroscopy. Journal of Luminescence, 2019, 215, 116615.	3.1	2
106	Ultra-low friction of a-C:H films enabled by lubrication of nanodiamond and graphene in ambient air. Carbon, 2019, 154, 203-210.	10.3	44
107	Mechanism of Superlubricity Conversion with Polyalkylene Glycol Aqueous Solutions. Langmuir, 2019, 35, 11784-11790.	3.5	22
108	Contribution of a Tribo-Induced Silica Layer to Macroscale Superlubricity of Hydrated Ions. Journal of Physical Chemistry C, 2019, 123, 20270-20277.	3.1	55

#	Article	IF	CITATIONS
109	In Situ Green Synthesis of the New Sandwichlike Nanostructure of Mn ₃ O ₄ /Graphene as Lubricant Additives. ACS Applied Materials & Interfaces, 2019, 11, 36931-36938.	8.0	55
110	Inâ€Plane Potential Gradient Induces Low Frictional Energy Dissipation during the Stick lip Sliding on the Surfaces of 2D Materials. Small, 2019, 15, e1904613.	10.0	19
111	Controllable Interlayer Charge and Energy Transfer in Perovskite Quantum Dots/ Transition Metal Dichalcogenide Heterostructures. Advanced Materials Interfaces, 2019, 6, 1901263.	3.7	17
112	Different directional energy dissipation of heterogeneous polymers in bimodal atomic force microscopy. RSC Advances, 2019, 9, 27464-27474.	3.6	5
113	The effect of magnetic field on the hydration of cation in solution revealed by THz spectroscopy and MDs. Colloids and Surfaces A: Physicochemical and Engineering Aspects, 2019, 582, 123822.	4.7	7
114	Fluorinated Graphene: A Promising Macroscale Solid Lubricant under Various Environments. ACS Applied Materials & Interfaces, 2019, 11, 40470-40480.	8.0	42
115	Macroscale superlubricity under extreme pressure enabled by the combination of graphene-oxide nanosheets with ionic liquid. Carbon, 2019, 151, 76-83.	10.3	86
116	Tribochemical Behaviors of Onion-like Carbon Films as High-Performance Solid Lubricants with Variable Interfacial Nanostructures. ACS Applied Materials & Interfaces, 2019, 11, 25535-25546.	8.0	46
117	Molecular behaviors in thin film lubrication—Part one: Film formation for different polarities of molecules. Friction, 2019, 7, 372-387.	6.4	29
118	Molecular behaviors in thin film lubrication—Part two: Direct observation of the molecular orientation near the solid surface. Friction, 2019, 7, 479-488.	6.4	30
119	Lubricity and Adsorption of Castor Oil Sulfated Sodium Salt Emulsion Solution on Titanium Alloy. Tribology Letters, 2019, 67, 1.	2.6	7
120	Superlubricity of Polyalkylene Glycol Aqueous Solutions Enabled by Ultrathin Layered Double Hydroxide Nanosheets. ACS Applied Materials & Interfaces, 2019, 11, 20249-20256.	8.0	62
121	Modeling Atomic-Scale Electrical Contact Quality Across Two-Dimensional Interfaces. Nano Letters, 2019, 19, 3654-3662.	9.1	21
122	Molecular Origin of Superlubricity between Graphene and a Highly Hydrophobic Surface in Water. Journal of Physical Chemistry Letters, 2019, 10, 2978-2984.	4.6	37
123	Crack Healing and Mechanical Properties Recovery in SA 508–3 Steel. Materials, 2019, 12, 890.	2.9	6
124	Friction and wear behavior of PTFE coatings modified with poly (methyl methacrylate). Composites Part B: Engineering, 2019, 172, 316-322.	12.0	47
125	Investigation of the lubrication properties and synergistic interaction of biocompatible liposome-polymer complexes applicable to artificial joints. Colloids and Surfaces B: Biointerfaces, 2019, 178, 469-478.	5.0	18
126	Core–shell nanospheres to achieve ultralow friction polymer nanocomposites with superior mechanical properties. Nanoscale, 2019, 11, 8237-8246.	5.6	29

#	Article	IF	CITATIONS
127	Exciton Radiative Recombination Dynamics and Nonradiative Energy Transfer in Two-Dimensional Transition-Metal Dichalcogenides. Journal of Physical Chemistry C, 2019, 123, 10087-10093.	3.1	31
128	A novel route to the synthesis of an Fe ₃ O ₄ /h-BN 2D nanocomposite as a lubricant additive. RSC Advances, 2019, 9, 6583-6588.	3.6	31
129	Molecular behaviors in thin film lubrication—Part three: Superlubricity attained by polar and nonpolar molecules. Friction, 2019, 7, 625-636.	6.4	49
130	Macroscale Superlubricity Achieved With Various Liquid Molecules: A Review. Frontiers in Mechanical Engineering, 2019, 5, .	1.8	46
131	Preparation of self-lubricating NiTi alloy and its self-adaptive behavior. Tribology International, 2019, 130, 43-51.	5.9	24
132	Synergistic tribological behaviors of graphene oxide and nanodiamond as lubricating additives in water. Tribology International, 2019, 132, 177-184.	5.9	65
133	Interlayer interaction on twisted interface in incommensurate stacking MoS2: A Raman spectroscopy study. Journal of Colloid and Interface Science, 2019, 538, 159-164.	9.4	15
134	Superlubricity and Antiwear Properties of In Situ-Formed Ionic Liquids at Ceramic Interfaces Induced by Tribochemical Reactions. ACS Applied Materials & Interfaces, 2019, 11, 6568-6574.	8.0	76
135	Microstructure, mechanical and adhesive properties of CrN/CrTiAlSiN/WCrTiAlN multilayer coatings deposited on nitrided AISI 4140 steel. Materials Characterization, 2019, 147, 353-364.	4.4	35
136	Gradual degeneration of liquid superlubricity: Transition from superlubricity to ordinary lubrication, and lubrication failure. Tribology International, 2019, 130, 352-358.	5.9	11
137	Effects of grain boundary on wear of graphene at the nanoscale: A molecular dynamics study. Carbon, 2019, 143, 578-586.	10.3	42
138	XPS and ToF-SIMS analysis of the tribochemical absorbed films on steel surfaces lubricated with diketone. Tribology International, 2019, 130, 184-190.	5.9	21
139	Water-based superlubricity in vacuum. Friction, 2019, 7, 192-198.	6.4	17
140	Tribological behavior of polytetrafluoroethylene coating reinforced with black phosphorus nanoparticles. Applied Surface Science, 2018, 441, 670-677.	6.1	53
141	Black phosphorus as a new lubricant. Friction, 2018, 6, 116-142.	6.4	136
142	Revealing the essence of luminescence energy transformation from silica surfaces. Journal of Luminescence, 2018, 197, 389-395.	3.1	1
143	Liquid Superlubricity of Polyethylene Glycol Aqueous Solution Achieved with Boric Acid Additive. Langmuir, 2018, 34, 3578-3587.	3.5	59
144	Laser irradiation-induced laminated graphene/MoS ₂ composites with synergistically improved tribological properties. Nanotechnology, 2018, 29, 265704.	2.6	26

#	Article	IF	CITATIONS
145	Nano-Ag-forest based surface enhanced Raman spectroscopy (SERS) of confined acetic acid. Colloids and Surfaces A: Physicochemical and Engineering Aspects, 2018, 547, 126-133.	4.7	8
146	Improvement of Load Bearing Capacity of Nanoscale Superlow Friction by Synthesized Fluorinated Surfactant Micelles. ACS Applied Nano Materials, 2018, 1, 953-959.	5.0	8
147	Superlubricity of Graphite Induced by Multiple Transferred Graphene Nanoflakes. Advanced Science, 2018, 5, 1700616.	11.2	99
148	Mechanism of Antiwear Property Under High Pressure of Synthetic Oil-Soluble Ultrathin MoS ₂ Sheets as Lubricant Additives. Langmuir, 2018, 34, 1635-1644.	3.5	43
149	Normal and Frictional Force Hysteresis between Selfâ€Assembled Fluorosurfactant Micelle Arrays at the Nanoscale. Advanced Materials Interfaces, 2018, 5, 1700802.	3.7	7
150	Superlubricity of 1-Ethyl-3-methylimidazolium trifluoromethanesulfonate Ionic Liquid Induced by Tribochemical Reactions. Langmuir, 2018, 34, 5245-5252.	3.5	47
151	Self-Lubricating PTFE-Based Composites with Black Phosphorus Nanosheets. Tribology Letters, 2018, 66, 1.	2.6	66
152	Friction-induced nano-structural evolution of graphene as a lubrication additive. Applied Surface Science, 2018, 434, 21-27.	6.1	175
153	Influence of the micromorphology of reduced graphene oxide sheets on lubrication properties as a lubrication additive. Tribology International, 2018, 119, 614-621.	5.9	60
154	Influence of annealing on the tribological properties of Zr-based bulk metallic glass. Journal of Non-Crystalline Solids, 2018, 481, 94-97.	3.1	19
155	Film forming behavior in thin film lubrication at high speeds. Friction, 2018, 6, 156-163.	6.4	17
156	Graphene Nanoflakes: Superlubricity of Graphite Induced by Multiple Transferred Graphene Nanoflakes (Adv. Sci. 3/2018). Advanced Science, 2018, 5, 1870018.	11.2	19
157	Water molecules on the liquid superlubricity interfaces achieved by phosphoric acid solution. Biosurface and Biotribology, 2018, 4, 94-98.	1.5	10
158	Self-Retraction of Surfactant Droplets on a Superhydrophilic Surface. Langmuir, 2018, 34, 15388-15395.	3.5	2
159	Dynamical characterization of micro cantilevers by different excitation methods in dynamic atomic force microscopy. Review of Scientific Instruments, 2018, 89, 115109.	1.3	6
160	Superlubricity of Black Phosphorus as Lubricant Additive. ACS Applied Materials & Interfaces, 2018, 10, 43203-43210.	8.0	113
161	Macroscale Superlubricity Enabled by the Synergy Effect of Graphene-Oxide Nanoflakes and Ethanediol. ACS Applied Materials & Interfaces, 2018, 10, 40863-40870.	8.0	131
162	Atomic Scale Simulation on the Fracture Mechanism of Black Phosphorus Monolayer under Indentation. Nanomaterials, 2018, 8, 682.	4.1	3

#	Article	IF	CITATIONS
163	Superlubricity of Graphite Sliding against Graphene Nanoflake under Ultrahigh Contact Pressure. Advanced Science, 2018, 5, 1800810.	11.2	85
164	Macroscale Superlubricity Enabled by Hydrated Alkali Metal Ions. Langmuir, 2018, 34, 11281-11291.	3.5	70
165	Random occurrence of macroscale superlubricity of graphite enabled by tribo-transfer of multilayer graphene nanoflakes. Carbon, 2018, 138, 154-160.	10.3	45
166	Layer-Number-Dependent Exciton Recombination Behaviors of MoS ₂ Determined by Fluorescence-Lifetime Imaging Microscopy. Journal of Physical Chemistry C, 2018, 122, 18651-18658.	3.1	21
167	Interlayer Friction and Superlubricity in Single-Crystalline Contact Enabled by Two-Dimensional Flake-Wrapped Atomic Force Microscope Tips. ACS Nano, 2018, 12, 7638-7646.	14.6	120
168	Black Phosphorus: Degradation Favors Lubrication. Nano Letters, 2018, 18, 5618-5627.	9.1	107
169	Superlubricity of 1,3-diketone based on autonomous viscosity control at various velocities. Tribology International, 2018, 126, 127-132.	5.9	27
170	Investigation of ultra-low friction on steel surfaces with diketone lubricants. RSC Advances, 2018, 8, 9402-9408.	3.6	12
171	Atomic Scale Simulation on the Anti-Pressure and Friction Reduction Mechanisms of MoS2 Monolayer. Materials, 2018, 11, 683.	2.9	8
172	Investigation on inner flow field characteristics of groove textures in fully lubricated thrust bearings. Industrial Lubrication and Tribology, 2018, 70, 754-763.	1.3	10
173	Fracture of the Intermolecular Hydrogen Bond Network Structure of Glycerol Modified by Carbon Nanotubes. Journal of Physical Chemistry C, 2018, 122, 19931-19936.	3.1	17
174	Origin of hydration lubrication of zwitterions on graphene. Nanoscale, 2018, 10, 16887-16894.	5.6	36
175	Tunable lubricity of aliphatic ammonium graphite intercalation compounds at the micro/nanoscale. Carbon, 2017, 115, 574-583.	10.3	8
176	Investigation of film formation mechanism of oil-in-water (O/W) emulsions at high speeds. Tribology International, 2017, 109, 428-434.	5.9	18
177	Enhanced phase and amplitude image contrasts of polymers in bimodal atomic force microscopy. RSC Advances, 2017, 7, 11768-11776.	3.6	15
178	Mild thermal reduction of graphene oxide as a lubrication additive for friction and wear reduction. RSC Advances, 2017, 7, 1766-1770.	3.6	41
179	Studies on triboluminescence emission characteristics of various kinds of bulk ZnS crystals. Journal of Luminescence, 2017, 186, 307-311.	3.1	10
180	Robust microscale superlubricity under high contact pressure enabled by graphene-coated microsphere. Nature Communications, 2017, 8, 14029.	12.8	235

#	Article	IF	CITATIONS
181	Increased Film Thickness of Oil-in-Water (O/W) Emulsions at High Speed. Tribology Letters, 2017, 65, 1.	2.6	1
182	Nonlinear Frictional Energy Dissipation between Silica-Adsorbed Surfactant Micelles. Journal of Physical Chemistry Letters, 2017, 8, 2258-2262.	4.6	18
183	Influence of interface interaction on the moir $ ilde{A}$ © superstructures of graphene on transition-metal substrates. RSC Advances, 2017, 7, 12179-12184.	3.6	10
184	Moiré superlattice-level stick-slip instability originated from geometrically corrugated graphene on a strongly interacting substrate. 2D Materials, 2017, 4, 025079.	4.4	33
185	Effect of liquid crystal molecular orientation controlled by an electric field on friction. Tribology International, 2017, 115, 477-482.	5.9	21
186	Self-Assembled Graphene Film as Low Friction Solid Lubricant in Macroscale Contact. ACS Applied Materials & Interfaces, 2017, 9, 21554-21562.	8.0	103
187	Tribological properties of titanium alloys under lubrication of SEE oil and aqueous solutions. Tribology International, 2017, 109, 40-47.	5.9	62
188	Numerical optimization of the groove texture bottom profile for thrust bearings. Tribology International, 2017, 109, 69-77.	5.9	47
189	Superlow Friction of Graphite Induced by the Self-Assembly of Sodium Dodecyl Sulfate Molecular Layers. Langmuir, 2017, 33, 12596-12601.	3.5	17
190	Tribological Behavior of NiAl-Layered Double Hydroxide Nanoplatelets as Oil-Based Lubricant Additives. ACS Applied Materials & Interfaces, 2017, 9, 30891-30899.	8.0	59
191	Imaging contrast and tip-sample interaction of non-contact amplitude modulation atomic force microscopy withQ-control. Journal Physics D: Applied Physics, 2017, 50, 415307.	2.8	4
192	Speed dependence of liquid superlubricity stability with H ₃ PO ₄ solution. RSC Advances, 2017, 7, 49337-49343.	3.6	13
193	Superlubricity of a graphene/MoS ₂ heterostructure: a combined experimental and DFT study. Nanoscale, 2017, 9, 10846-10853.	5.6	133
194	Synthesis of thermally reduced graphite oxide in sulfuric acid and its application as an efficient lubrication additive. Tribology International, 2017, 116, 303-309.	5.9	58
195	Triboluminescence modulated by humidity. Journal of Luminescence, 2017, 182, 22-28.	3.1	11
196	Evolution of tribo-induced interfacial nanostructures governing superlubricity in a-C:H and a-C:H:Si films. Nature Communications, 2017, 8, 1675.	12.8	179
197	Interfacial interaction and enhanced image contrasts in higher mode and bimodal mode atomicÂforce microscopy. RSC Advances, 2017, 7, 55121-55130.	3.6	5
198	Dramatically Enhanced Film-Formation Performance Using O/W Emulsion Under Starving Feeding Mode. Tribology Letters, 2017, 65, 1.	2.6	1

#	Article	IF	CITATIONS
199	Guest editorial: Special issue on 6th World Tribology Congress. Friction, 2017, 5, 231-232.	6.4	0
200	Signal processing and analysis for copper layer thickness measurement within a large variation range in the CMP process. Review of Scientific Instruments, 2017, 88, 115103.	1.3	5
201	Motor Power Signal Analysis for End-Point Detection of Chemical Mechanical Planarization. Micromachines, 2017, 8, 177.	2.9	7
202	Effect of Parameters on Internal Crack Healing in 30Cr2Ni4MoV Steel for 600-Ton Ultra-Super Ingots. Metals, 2017, 7, 149.	2.3	10
203	Hot Deformation Behavior of As-Cast 30Cr2Ni4MoV Steel Using Processing Maps. Metals, 2017, 7, 50.	2.3	7
204	Triboluminescence dominated by crystallographic orientation. Scientific Reports, 2016, 6, 26324.	3.3	2
205	Thin film lubrication in the past 20 years. Friction, 2016, 4, 280-302.	6.4	70
206	Effects of interfacial alignments on the stability of graphene on Ru(0001) substrate. Applied Physics Letters, 2016, 108, .	3.3	15
207	Effect of Alkyl Chain Length on the Orientational Behavior of Liquid Crystals Nano-Film. Tribology Letters, 2016, 62, 1.	2.6	11
208	Influence of tribofilm on superlubricity of highly-hydrogenated amorphous carbon films in inert gaseous environments. Science China Technological Sciences, 2016, 59, 1795-1803.	4.0	20
209	Highly Exfoliated Reduced Graphite Oxide Powders as Efficient Lubricant Oil Additives. Advanced Materials Interfaces, 2016, 3, 1600700.	3.7	59
210	Size and shape controllable preparation of graphene sponge by freezing, lyophilizing and reducing in container. Science China Technological Sciences, 2016, 59, 709-713.	4.0	4
211	Expressions for the evaporation of sessile liquid droplets incorporating the evaporative cooling effect. Journal of Colloid and Interface Science, 2016, 484, 291-297.	9.4	14
212	Investigation of Superlubricity Achieved by Polyalkylene Glycol Aqueous Solutions. Advanced Materials Interfaces, 2016, 3, 1600531.	3.7	37
213	Layered Double Hydroxide Nanoplatelets with Excellent Tribological Properties under High Contact Pressure as Water-Based Lubricant Additives. Scientific Reports, 2016, 6, 22748.	3.3	41
214	Robust ultra-low-friction state of graphene via moiré superlattice confinement. Nature Communications, 2016, 7, 13204.	12.8	116
215	Guest editorial: Special issue on thin film lubrication. Friction, 2016, 4, 277-279.	6.4	1
216	Effect of Potassium lons on Tantalum Chemical Mechanical Polishing in H ₂ O ₂ -Based Alkaline Slurries. ECS Journal of Solid State Science and Technology, 2016, 5, P100-P111.	1.8	8

#	Article	IF	CITATIONS
217	AFM Studies on Liquid Superlubricity between Silica Surfaces Achieved with Surfactant Micelles. Langmuir, 2016, 32, 5593-5599.	3.5	55
218	Passivation Kinetics of 1,2,4-Triazole in Copper Chemical Mechanical Polishing. ECS Journal of Solid State Science and Technology, 2016, 5, P272-P279.	1.8	17
219	Investigation of running-in process in water-based lubrication aimed at achieving super-low friction. Tribology International, 2016, 102, 257-264.	5.9	49
220	An experimental investigation of double-side processing of cylindrical rollers using chemical mechanical polishing technique. International Journal of Advanced Manufacturing Technology, 2016, 82, 523-534.	3.0	15
221	An investigation on the tribological properties of multilayer graphene and MoS2 nanosheets as additives used in hydraulic applications. Tribology International, 2016, 97, 14-20.	5.9	193
222	Tribological properties of few-layer graphene oxide sheets as oil-based lubricant additives. Chinese Journal of Mechanical Engineering (English Edition), 2016, 29, 439-444.	3.7	29
223	Superlubricity of nanodiamonds glycerol colloidal solution between steel surfaces. Colloids and Surfaces A: Physicochemical and Engineering Aspects, 2016, 489, 400-406.	4.7	43
224	Friction Anisotropy Induced by Oriented Liquid Crystal Molecules. Tribology Letters, 2016, 61, 1.	2.6	10
225	Friction and wear performance of titanium alloy against tungsten carbide lubricated with phosphate ester. Tribology International, 2016, 95, 27-34.	5.9	63
226	Ultrathin MoS2 Nanosheets with Superior Extreme Pressure Property as Boundary Lubricants. Scientific Reports, 2015, 5, 12869.	3.3	140
227	Tip-induced nanoreactor for silicate. Scientific Reports, 2015, 5, 14039.	3.3	0
228	Advances in thin film lubrication (TFL): From discovery to the aroused further researches. Science China Technological Sciences, 2015, 58, 1609-1616.	4.0	8
229	Interface characteristics of thin liquid films in a charged lubricated contact. Surface and Interface Analysis, 2015, 47, 315-324.	1.8	2
230	Experimental Investigation of Centrifugal Effects on Lubricant Replenishment in the Starved Regime at High Speeds. Tribology Letters, 2015, 59, 1.	2.6	28
231	Tribochemical Mechanism of Amorphous Silica Asperities in Aqueous Environment: A Reactive Molecular Dynamics Study. Langmuir, 2015, 31, 1429-1436.	3.5	54
232	Pitted Surfaces Produced by Lactic Acid Lubrication and Their Effect on Ultra-Low Friction. Tribology Letters, 2015, 57, 1.	2.6	9
233	The film forming behavior at high speeds under oilâ^'air lubrication. Tribology International, 2015, 91, 6-13.	5.9	27
234	Investigation of the difference in liquid superlubricity between water- and oil-based lubricants. RSC Advances, 2015, 5, 63827-63833.	3.6	62

#	Article	IF	CITATIONS
235	Combined effects of underlying substrate and evaporative cooling on the evaporation of sessile liquid droplets. Soft Matter, 2015, 11, 5632-5640.	2.7	26
236	Superlubricity of silicone oil achieved between two surfaces by running-in with acid solution. RSC Advances, 2015, 5, 30861-30868.	3.6	53
237	Chemical mechanical polishing of steel substrate using colloidal silica-based slurries. Applied Surface Science, 2015, 330, 487-495.	6.1	45
238	Chemical Mechanical Polishing of Stainless Steel as Solar Cell Substrate. ECS Journal of Solid State Science and Technology, 2015, 4, P162-P170.	1.8	19
239	Lubrication under charged conditions. Tribology International, 2015, 84, 22-35.	5.9	56
240	Influence of thermal effects on elastohydrodynamic (EHD) lubrication behavior at high speeds. Science China Technological Sciences, 2015, 58, 551-558.	4.0	14
241	Experimental Investigation of Lubrication Film Starvation of Polyalphaolefin Oil at High Speeds. Tribology Letters, 2014, 56, 491-500.	2.6	24
242	Temperature distribution along the surface of evaporating droplets. Physical Review E, 2014, 89, 032404.	2.1	47
243	<i>In situ</i> observation of the molecular ordering in the lubricating point contact area. Journal of Applied Physics, 2014, 116, .	2.5	16
244	Effects of pH and Oxidizer on Chemical Mechanical Polishing of AISI 1045 Steel. Tribology Letters, 2014, 56, 327-335.	2.6	9
245	Reemulsification effect on the film formation of O/W emulsion. Journal of Colloid and Interface Science, 2014, 417, 238-243.	9.4	18
246	Synergetic effect of benzotriazole and non-ionic surfactant on copper chemical mechanical polishing in KIO4-based slurries. Thin Solid Films, 2014, 558, 272-278.	1.8	50
247	Insight into the formation mechanism of durable hexadecylphosphonic acid bilayers on titanium alloy through interfacial analysis. Colloids and Surfaces A: Physicochemical and Engineering Aspects, 2014, 447, 51-58.	4.7	13
248	1,2,4-Triazole as a corrosion inhibitor in copper chemical mechanical polishing. Thin Solid Films, 2014, 556, 395-404.	1.8	73
249	Mechanical properties of nanoparticles: basics and applications. Journal Physics D: Applied Physics, 2014, 47, 013001.	2.8	454
250	Functions of Trilon® P as a polyamine in copper chemical mechanical polishing. Applied Surface Science, 2014, 288, 265-274.	6.1	35
251	Superlubricity of two-dimensional fluorographene/MoS ₂ heterostructure: a first-principles study. Nanotechnology, 2014, 25, 385701.	2.6	98
252	Effect of pH on the liquid superlubricity between Si ₃ N ₄ and glass achieved with phosphoric acid. RSC Advances, 2014, 4, 45735-45741.	3.6	10

#	Article	IF	CITATIONS
253	Direct observation of the formation and destruction of the inverted continuous oil phase in the micro-outlet region achieved by the confined diluted O/W emulsion stream. Soft Matter, 2014, 10, 7946-7951.	2.7	5
254	Ultra-low friction achieved by diluted lactic acid solutions. RSC Advances, 2014, 4, 28860.	3.6	10
255	Mechanical Properties and Interface Characteristics of Nanoporous Low- <i>k</i> Materials. ACS Applied Materials & Interfaces, 2014, 6, 13850-13858.	8.0	19
256	Mechanism of Biological Liquid Superlubricity of <i>Brasenia schreberi</i> Mucilage. Langmuir, 2014, 30, 3811-3816.	3.5	45
257	The Assessment of Interface Adhesion of Cu/Ta/Black Diamondâ,,¢/Si Films Stack Structure by Nanoindentation and Nanoscratch Tests. Tribology Letters, 2014, 53, 401-410.	2.6	4
258	Investigations of the superlubricity of sapphire against ruby under phosphoric acid lubrication. Friction, 2014, 2, 164-172.	6.4	40
259	Hydrodynamic effect on the superlubricity of phosphoric acid between ceramic and sapphire. Friction, 2014, 2, 173-181.	6.4	58
260	Guest editorial: Special issue on superlubricity. Friction, 2014, 2, 93-94.	6.4	4
261	Interfacial Dynamics and Adhesion Behaviors of Water and Oil Droplets in Confined Geometry. Langmuir, 2014, 30, 7695-7702.	3.5	5
262	Effect of ionic strength on ruthenium CMP in H2O2-based slurries. Applied Surface Science, 2014, 317, 332-337.	6.1	69
263	Linear growth of colloidal rings at the edge of drying droplets. Colloids and Surfaces A: Physicochemical and Engineering Aspects, 2014, 447, 28-31.	4.7	12
264	Elastic Properties of Polystyrene Nanospheres Evaluated with Atomic Force Microscopy: Size Effect and Error Analysis. Langmuir, 2014, 30, 7206-7212.	3.5	75
265	Synergetic effect of H2O2 and glycine on cobalt CMP in weakly alkaline slurry. Microelectronic Engineering, 2014, 122, 82-86.	2.4	82
266	Investigation on the galvanic corrosion of copper during chemical mechanical polishing of ruthenium barrier layer. , 2014, , .		6
267	Reduction of friction stress of ethylene glycol by attached hydrogen ions. Scientific Reports, 2014, 4, 7226.	3.3	23
268	Superlubricity Achieved with Mixtures of Polyhydroxy Alcohols and Acids. Langmuir, 2013, 29, 5239-5245.	3.5	92
269	Stress analysis of Cu/low-k interconnect structure during whole Cu-CMP process using finite element method. Microelectronics Reliability, 2013, 53, 767-773.	1.7	6
270	Superlubricity of Si3N4 sliding against SiO2 under linear contact conditions in phosphoric acid solutions. Science China Technological Sciences, 2013, 56, 1678-1684.	4.0	19

#	Article	IF	CITATIONS
271	Achievement of a near-perfect smooth silicon surface. Science China Technological Sciences, 2013, 56, 2847-2853.	4.0	23
272	Damages on the lubricated surfaces in bearings under the influence of weak electrical currents. Science China Technological Sciences, 2013, 56, 2979-2987.	4.0	11
273	Advancements in superlubricity. Science China Technological Sciences, 2013, 56, 2877-2887.	4.0	54
274	Analysis of Measurement Inaccuracy in Superlubricity Tests. Tribology Transactions, 2013, 56, 141-147.	2.0	30
275	Electrochemical investigation of copper passivation kinetics and its application to low-pressure CMP modeling. Applied Surface Science, 2013, 265, 764-770.	6.1	39
276	Material Removal Mechanism of Copper CMP from a Chemical–Mechanical Synergy Perspective. Tribology Letters, 2013, 49, 11-19.	2.6	29
277	Failure analysis of journal bearing used in turboset of a power plant. Materials & Design, 2013, 52, 923-931.	5.1	28
278	Optimization of design of experiment for chemical mechanical polishing of a 12-inch wafer. Microelectronic Engineering, 2013, 112, 5-9.	2.4	12
279	Wafer bending/orientation characterization and their effects on fluid lubrication during chemical mechanical polishing. Tribology International, 2013, 66, 330-336.	5.9	5
280	A comparative study between graphene oxide and diamond nanoparticles as water-based lubricating additives. Science China Technological Sciences, 2013, 56, 152-157.	4.0	63
281	AC Pulse Dielectric Barrier Corona Discharge Over Oil Surfaces: Effect of Oil Temperature. IEEE Transactions on Plasma Science, 2013, 41, 481-484.	1.3	6
282	Measurement of the Friction between Single Polystyrene Nanospheres and Silicon Surface Using Atomic Force Microscopy. Langmuir, 2013, 29, 6920-6925.	3.5	15
283	Aminosilanization Nanoadhesive Layer for Nanoelectric Circuits with Porous Ultralow Dielectric Film. ACS Applied Materials & Interfaces, 2013, 5, 6097-6107.	8.0	17
284	Superlubricity Achieved with Mixtures of Acids and Glycerol. Langmuir, 2013, 29, 271-275.	3.5	126
285	Tribochemistry of Phosphoric Acid Sheared between Quartz Surfaces: A Reactive Molecular Dynamics Study. Journal of Physical Chemistry C, 2013, 117, 25604-25614.	3.1	55
286	Controllable Superlubricity of Glycerol Solution via Environment Humidity. Langmuir, 2013, 29, 11924-11930.	3.5	50
287	Investigation of Protein Adsorption Mechanism and Biotribological Properties at Simulated Stem-Cement Interface. Journal of Tribology, 2013, 135, .	1.9	30
288	Investigations on the mechanism of superlubricity achieved with phosphoric acid solution by direct observation. Journal of Applied Physics, 2013, 114, 114901.	2.5	34

#	Article	IF	CITATIONS
289	Effects of the Polishing Variables on the Wafer-Pad Interfacial Fluid Pressure in Chemical Mechanical Polishing of 12-Inch Wafer. Journal of the Electrochemical Society, 2012, 159, H342-H348.	2.9	9
290	The Role of Hydroxyethyl Cellulose (HEC) in the Chemical Mechanical Planarization of Copper. Journal of the Electrochemical Society, 2012, 159, H329-H334.	2.9	11
291	Direct observation on the behaviour of emulsion droplets and formation of oil pool under point contact. Applied Physics Letters, 2012, 101, .	3.3	10
292	"Boiling―in the water evaporating meniscus induced by Marangoni flow. Applied Physics Letters, 2012, 101, .	3.3	8
293	Water droplets on a hydrophobic insulator surface under high voltages: A thermal perspective. Applied Physics Letters, 2012, 101, 131602.	3.3	9
294	Superlubricity Mechanism of Brasenia Schreberi Mucilage. , 2012, , .		0
295	Friction Process of Superlubricity. , 2012, , .		1
296	Radial-velocity profile along the surface of evaporating liquid droplets. Soft Matter, 2012, 8, 5797.	2.7	31
297	Planarization process of single crystalline silicon asperity under abrasive rolling effect studied by molecular dynamics simulation. Applied Physics A: Materials Science and Processing, 2012, 109, 119-126.	2.3	16
298	Investigation on growth process and tribological behavior of mixed alkylsilane self-assembled molecular films in aqueous solution. Applied Surface Science, 2012, 258, 8533-8537.	6.1	5
299	A flexible nanobrush pad for the chemical mechanical planarization of Cu/ultra-low-к materials. Nanoscale Research Letters, 2012, 7, 603.	5.7	2
300	Tribochemistry and Superlubricity Induced by Hydrogen Ions. Langmuir, 2012, 28, 15816-15823.	3.5	83
301	Modification on the tribological properties of ceramics lubricated by water using fullerenol as a lubricating additive. Science China Technological Sciences, 2012, 55, 2656-2661.	4.0	23
302	Preparation of poly (N-isopropylacrylamide) brush bonded on silicon substrate and its water-based lubricating property. Science China Technological Sciences, 2012, 55, 3352-3358.	4.0	12
303	Excellent Lubricating Behavior of Brasenia schreberi Mucilage. Langmuir, 2012, 28, 7797-7802.	3.5	74
304	Behavior of O/W Emulsion Under Point Contact. , 2012, , .		0
305	Film formation of yogurt under confined condition. Surface and Interface Analysis, 2012, 44, 258-262.	1.8	1
306	Effect of crystallographic orientation on the extrusion of silicon surface during an impact: Molecular dynamics simulation. Nuclear Instruments & Methods in Physics Research B, 2012, 270, 133-139.	1.4	4

#	Article	IF	CITATIONS
307	Effects of Chemical Additives of CMP Slurry on Surface Mechanical Characteristics and Material Removal of Copper. Tribology Letters, 2012, 45, 309-317.	2.6	29
308	Electrospreading of dielectric liquid menisci on the small scale. Soft Matter, 2011, 7, 6076.	2.7	12
309	Nanoconfined liquid aliphatic compounds under external electric fields: roles of headgroup and alkyl chain length. Soft Matter, 2011, 7, 4453.	2.7	14
310	Investigation of the film formation mechanism of oil-in-water (O/W) emulsions. Soft Matter, 2011, 7, 4207.	2.7	32
311	Superlubricity Behavior with Phosphoric Acid–Water Network Induced by Rubbing. Langmuir, 2011, 27, 9413-9417.	3.5	173
312	Comparison of surface damage under the dry and wet impact: Molecular dynamics simulation. Applied Surface Science, 2011, 258, 1756-1761.	6.1	24
313	Preparation, Characterization and Formation Mechanism of Thermoplastic Polyurethane Nanostructures Using Solution Wetting Template. Journal of Nanoscience and Nanotechnology, 2011, 11, 10240-10246.	0.9	3
314	Direct observation of oil displacement by water flowing toward an oil nanogap. Journal of Applied Physics, 2011, 110, 044906.	2.5	3
315	A lubrication model between the soft porous brush and rigid flat substrate for post-CMP cleaning. Microelectronic Engineering, 2011, 88, 2862-2870.	2.4	15
316	Modeling of particle removal processes in brush scrubber cleaning. Wear, 2011, 273, 105-110.	3.1	18
317	Influence of pH, immersion time, and benzotriazole concentration on copper corrosion in citric acid based slurries. Science Bulletin, 2011, 56, 1158-1164.	1.7	2
318	Effects of the ultrasonic flexural vibration on the interaction between the abrasive particles; pad and sapphire substrate during chemical mechanical polishing (CMP). Applied Surface Science, 2011, 257, 2905-2911.	6.1	66
319	Mechanisms for nano particle removal in brush scrubber cleaning. Applied Surface Science, 2011, 257, 3055-3062.	6.1	32
320	Nanoparticle–wall collision in a laminar cylindrical liquid jet. Journal of Colloid and Interface Science, 2011, 359, 334-338.	9.4	16
321	Thin liquid film lubrication under external electrical fields: Roles of liquid intermolecular interactions. Journal of Applied Physics, 2011, 109, .	2.5	11
322	Abrasive rolling effects on material removal and surface finish in chemical mechanical polishing analyzed by molecular dynamics simulation. Journal of Applied Physics, 2011, 109, .	2.5	47
323	Electrical potential modulation of dynamic film properties of aqueous surfactant solutions through a nanogap. Journal of Applied Physics, 2011, 109, 024309.	2.5	2
324	Probing Particle Movement in CMP with Fluorescence Technique. Journal of the Electrochemical Society, 2011, 158, H681.	2.9	14

#	Article	IF	CITATIONS
325	Modeling the Chemical-Mechanical Synergy during Copper CMP. Journal of the Electrochemical Society, 2011, 158, H197.	2.9	19
326	Advancements and Future of Tribology from IFToMM. Mechanisms and Machine Science, 2011, , 203-219.	0.5	0
327	The Film Formation Mechanism of High Water-Based Emulsions. , 2010, , .		0
328	The Film Behaviors of Grease in Point Contact During Microoscillation. Tribology Letters, 2010, 38, 259-266.	2.6	11
329	Experimental Investigation of Lubrication Properties at High Contact Pressure. Tribology Letters, 2010, 40, 85-97.	2.6	11
330	Effect of solid surface on the formation of thin confined lubricating film of water with micro-content of oil. Applied Surface Science, 2010, 256, 6574-6579.	6.1	8
331	Ultrasonic flexural vibration assisted chemical mechanical polishing for sapphire substrate. Applied Surface Science, 2010, 256, 3936-3940.	6.1	77
332	Nanoconfined ionic liquids under electric fields. Applied Physics Letters, 2010, 96, .	3.3	73
333	Monoatomic layer removal mechanism in chemical mechanical polishing process: A molecular dynamics study. Journal of Applied Physics, 2010, 107, .	2.5	56
334	Dynamic phase transformation of crystalline silicon under the dry and wet impact studied by molecular dynamics simulation. Journal of Applied Physics, 2010, 108, .	2.5	10
335	Bubble generation in a nanoconfined liquid film between dielectric-coated electrodes under alternating current electric fields. Applied Physics Letters, 2010, 96, .	3.3	14
336	Performance of Sodium Dodecyl Sulfate in Slurry with Glycine and Hydrogen Peroxide for Copper-Chemical Mechanical Polishing. Journal of the Electrochemical Society, 2010, 157, H1082.	2.9	21
337	Electric-fields-enhanced destabilization of oil-in-water emulsions flowing through a confined wedgelike gap. Journal of Applied Physics, 2010, 108, 064314.	2.5	7
338	"Freezing―of Nanoconfined Fluids under an Electric Field. Langmuir, 2010, 26, 1445-1448.	3.5	23
339	Criterion for Reversal of Thermal Marangoni Flow in Drying Drops. Langmuir, 2010, 26, 1918-1922.	3.5	96
340	Effect of microcontent of oil in water under confined condition. Applied Physics Letters, 2009, 95, 091908.	3.3	15
341	Energy transfer under impact load studied by molecular dynamics simulation. Journal of Nanoparticle Research, 2009, 11, 589-600.	1.9	15
342	Film-forming Characteristics of Grease in Point Contact under Swaying Motions. Tribology Letters, 2009, 35, 57-65.	2.6	14

#	Article	IF	CITATIONS
343	Study of lubrication behavior of pure water for hydrophobic friction pair. Science in China Series D: Earth Sciences, 2009, 52, 3128-3134.	0.9	3
344	A comparative study of tribological properties between perfluoro and non-perfluoro alkylsilane self-assembled monolayers(SAMs). Journal Wuhan University of Technology, Materials Science Edition, 2009, 24, 588-593.	1.0	3
345	Film forming characteristics of oil-in-water emulsion with super-low oil concentration. Colloids and Surfaces A: Physicochemical and Engineering Aspects, 2009, 340, 70-76.	4.7	28
346	Investigation of the running-in process and friction coefficient under the lubrication of ionic liquid/water mixture. Applied Surface Science, 2009, 255, 6408-6414.	6.1	35
347	Particles detection and analysis of hard disk substrate after cleaning of post chemical mechanical polishing. Applied Surface Science, 2009, 255, 9100-9104.	6.1	19
348	The protective properties of ultra-thin diamond like carbon films for high density magnetic storage devices. Applied Surface Science, 2009, 256, 322-328.	6.1	37
349	Effect of surface charge on water film nanoconfined between hydrophilic solid surfaces. Journal of Applied Physics, 2009, 105, 124301.	2.5	21
350	Tribology in Nanomanufacturing—Interaction between Nanoparticles and a Solid Surface. , 2009, , 5-10.		2
351	Effect of surface physicochemical properties on the lubricating properties of water film. Applied Surface Science, 2008, 254, 7137-7142.	6.1	43
352	Micro-Bubble Phenomenon in Nanoscale Water-based Lubricating Film Induced by External Electric Field. Tribology Letters, 2008, 29, 169-176.	2.6	25
353	Nanotube–Silicon Heterojunction Solar Cells. Advanced Materials, 2008, 20, 4594-4598.	21.0	210
354	Effect of substrate morphology on the roughness evolution of ultra thin DLC films. Applied Surface Science, 2008, 254, 6742-6748.	6.1	41
355	Mechanical properties of La2O3 doped diamond-like carbon films. Surface and Coatings Technology, 2008, 202, 1621-1627.	4.8	18
356	Preparation of α-alumina-g-polyacrylamide composite abrasive and chemical mechanical polishing behavior. Thin Solid Films, 2008, 516, 3005-3008.	1.8	29
357	Phase transformation during silica cluster impact on crystal silicon substrate studied by molecular dynamics simulation. Nuclear Instruments & Methods in Physics Research B, 2008, 266, 3231-3240.	1.4	10
358	Effect of Nanoparticle Impact on Material Removal. Tribology Transactions, 2008, 51, 718-722.	2.0	16
359	Microstructure and mechanical properties of CeO2 doped diamond-like carbon films. Diamond and Related Materials, 2008, 17, 396-404.	3.9	16
360	A PIV system for two-phase flow with nanoparticles. International Journal of Surface Science and Engineering, 2008, 2, 168.	0.4	7

#	Article	IF	CITATIONS
361	Extrusion formation mechanism on silicon surface under the silica cluster impact studied by molecular dynamics simulation. Journal of Applied Physics, 2008, 104, .	2.5	30
362	Synergistic Effect of Ethylene Thiourea and Bis-(3-sulfopropyl)-disulfide on Acid Cu Electrodeposition. Journal of the Electrochemical Society, 2007, 154, D526.	2.9	11
363	Marangoni flow in an evaporating water droplet. Applied Physics Letters, 2007, 91, .	3.3	248
364	Preparation and characterization of La2O3 doped diamond-like carbon nanofilms (I): Structure analysis. Diamond and Related Materials, 2007, 16, 1905-1911.	3.9	26
365	Double-Walled Carbon Nanotube Solar Cells. Nano Letters, 2007, 7, 2317-2321.	9.1	321
366	Characteristics of thin liquid film under an external electric field. Tribology International, 2007, 40, 1718-1723.	5.9	3
367	The effect of sulfur on the number of layers in a carbon nanotube. Carbon, 2007, 45, 2152-2158.	10.3	68
368	Rare earth effect on the microstructure and wear resistance of Ni-based coatings. Materials Science & Engineering A: Structural Materials: Properties, Microstructure and Processing, 2007, 454-455, 194-202.	5.6	55
369	Rare earth effect on microstructure, mechanical and tribological properties of CoCrW coatings. Materials Science & Engineering A: Structural Materials: Properties, Microstructure and Processing, 2007, 444, 92-98.	5.6	57
370	Spread of double-walled carbon nanotube membrane. Science Bulletin, 2007, 52, 997-1000.	1.7	5
371	Tribological properties of La2O3 and CeO2 doped CoCrW coatings deposited by supersonic plasma spraying. Science Bulletin, 2007, 52, 3292-3298.	1.7	10
372	Luminescence of carbon nanotube bulbs. Science Bulletin, 2007, 52, 113-117.	1.7	9
373	Tribological properties of rare earth oxide added Cr3C2–NiCr coatings. Applied Surface Science, 2007, 253, 4377-4385.	6.1	43
374	Analysis on contact and flow features in CMP process. Science Bulletin, 2006, 51, 2281-2286.	1.7	9
375	Light-induced Current in Long Carbon Nanotubes. ECS Transactions, 2006, 2, 85-92.	0.5	0
376	Gas bubble phenomenon in nanoscale liquid film under external electric field. Applied Physics Letters, 2006, 89, 013104.	3.3	22
377	Analysis on mechanism of thin film lubrication. Science Bulletin, 2005, 50, 2645-2649.	1.7	4
378	Progress in material removal mechanisms of surface polishing with ultra precision. Science Bulletin, 2004, 49, 1687-1693.	1.7	22

#	Article	IF	CITATIONS
379	CMP of hard disk substrate using a colloidal SiO2 slurry: preliminary experimental investigation. Wear, 2004, 257, 461-470.	3.1	123
380	The experimental rules of mica as a reference sample of AFM/FFM measurement. Science Bulletin, 2001, 46, 349-352.	1.7	7
381	Nano-tribological properties and mechanisms of the liquid crystal as an additive. Science Bulletin, 2001, 46, 1227-1232.	1.7	35
382	Tribological properties of OTS self-assembled monolayers. Science Bulletin, 2001, 46, 698-701.	1.7	8
383	Effects of surface physicochemical properties on the tribological properties of liquid paraffin film in the nanoscale. Surface and Interface Analysis, 2001, 32, 286-288.	1.8	9
384	The Tribological Properties of Oils Added with Diamond Nano-Particles. Tribology Transactions, 2001, 44, 494-498.	2.0	88
385	THIN FILM LUBRICATION AND LUBRICATION MAP. Jixie Gongcheng Xuebao/Chinese Journal of Mechanical Engineering, 2000, 36, 5.	0.5	11
386	Characteristics of Liquid Lubricant Films at the Nano-Scale. Journal of Tribology, 1999, 121, 872-878.	1.9	40
387	The Failure of Fluid Film at Nano-Scale. Tribology Transactions, 1999, 42, 912-916.	2.0	30
388	Progresses and problems in nano-tribology. Science Bulletin, 1998, 43, 369-378.	1.7	14
389	Thin film lubrication. Part I. Study on the transition between EHL and thin film lubrication using a relative optical interference intensity technique. Wear, 1996, 194, 107-115.	3.1	270
390	Tribological and compressive creep properties of polytetrafluoroethylene/nickelâ€ŧitanium shape memory alloy composites. Polymer Composites, 0, , .	4.6	6